

1        **Transient and quasi-equilibrium climate states at 1.5°C and 2°C global warming**

2        Andrew D. King<sup>1,2</sup>, Alexander R. Borowiak<sup>1,2</sup>, Josephine R. Brown<sup>1,2</sup>, David J. Frame<sup>3</sup>, Luke  
3        J. Harrington<sup>3</sup>, Seung-Ki Min<sup>4,5</sup>, Angeline Pendergrass<sup>6,7</sup>, Maria Rugenstein<sup>8</sup>, J. M. Kale  
4        Sniderman<sup>1</sup>, Dáithí A. Stone<sup>9</sup>

5        1. School of Earth Sciences, University of Melbourne, Melbourne, Victoria, Australia.

6        2. ARC Centre of Excellence for Climate Extremes, University of Melbourne,  
7        Melbourne, Victoria, Australia.

8        3. New Zealand Climate Change Research Institute, School of Geography, Environment  
9        and Earth Sciences, Victoria University of Wellington, Wellington, New Zealand.

10       4. Division of Environmental Science and Engineering, Pohang University of Science  
11       and Technology, Pohang, South Korea

12       5. Institute for Convergence Research and Education in Advanced Technology, Yonsei  
13       University, Incheon, South Korea

14       6. Cornell University, Ithaca, NY, USA.

15       7. National Center for Atmospheric Research, Boulder, Colorado, USA

16       8. Department of Atmospheric Science, Colorado State University, Fort Collins,  
17       Colorado, USA.

18       9. NIWA, Wellington, New Zealand

19

20       **Key points**

21       • Warming patterns at Paris Agreement limits differ substantially between transient and  
22       quasi-equilibrium climates

23       • Summer climate changes over northern land are clearer in a transient climate than a  
24       stabilised climate at the same global warming level

- 25 • Projections of regional climate designed for the Paris Agreement limits are only
- 26 useful if the rate of global warming is explicit
- 27 Email: [andrew.king@unimelb.edu.au](mailto:andrew.king@unimelb.edu.au)

## 28 **Abstract**

29 Recent climate change is characterised by rapid global warming, but the goal of the Paris  
30 Agreement is to achieve a stable climate where global temperatures remain well below 2°C  
31 above pre-industrial levels. Inferences about conditions at or below 2°C are usually made  
32 based on transient climate projections. To better understand climate change impacts on  
33 natural and human systems under the Paris Agreement, we must understand how a stable  
34 climate may differ from transient conditions at the same warming level. Here we examine  
35 differences between transient and quasi-equilibrium climates based on greenhouse gas-only  
36 model simulations at 1.5°C and 2°C global warming. We find substantial local differences  
37 between seasonal-average temperatures, with mid-latitude land regions in boreal summer  
38 considerably warmer in a transient climate than a quasi-equilibrium state at both 1.5°C and  
39 2°C global warming. Our research demonstrates that the rate of global warming must be  
40 considered in regional projections.

## 41 **Plain language summary**

42 The world has warmed quickly since around 1970, prompting efforts to mitigate climate  
43 change and to stabilise global temperatures between 1.5°C and 2°C above pre-industrial  
44 levels. We explore the differences between a rapidly-warming climate and one with little  
45 change in global temperature over time. We find that a fast-warming climate is characterised  
46 by warmer temperatures over Northern Hemisphere mid-latitude land regions than a stable  
47 climate at the same level of global warming. The opposite is true in the Southern Ocean  
48 where slower warming occurs because of the lag in warming of the deep ocean, so as the  
49 global climate stabilises that region continues to warm. As the world continues to warm,  
50 some land locations, such as the interior of North America and Eurasia, may experience a  
51 temporary emergence of a climate change signal that weakens if the climate stabilises and the

52 Paris Agreement goals are met. The difference between fast-warming and stable climates can  
53 be very large locally, so they must be considered in planning for adapting to future climate  
54 change.

## 55 **Introduction**

56 The planet is warming rapidly and, to date, has already warmed around 1.2°C relative to  
57 early-industrial levels due to human influences (Haustein et al., 2017). In an effort to reduce  
58 the impacts of climate change, the Paris Agreement was developed with the aim of limiting  
59 global warming to well below 2°C and preferably below 1.5°C above pre-industrial levels.  
60 Since 2015, when the Paris Agreement was developed, there have been many studies  
61 examining climate impacts at different global warming levels (GWLs) to quantify the  
62 benefits of limiting global warming. A variety of methods are used to generate quantitative  
63 estimates of climate change impacts at different GWLs, including time-slicing of existing  
64 model simulations (Schleussner et al., 2016), development of single coupled-model  
65 ensembles at GWLs (Sanderson et al., 2017), development of multi-model atmosphere-only  
66 ensembles (Mitchell et al., 2017), and pattern scaling (Seneviratne et al., 2016; Tebaldi &  
67 Knutti, 2018). These methods are described in James et al. (2017) and Masson-Delmotte et  
68 al., (2018). The methods listed above describe worlds at given GWLs with different rates of  
69 warming. For example, many studies have used time-slicing from rapid-warming scenarios  
70 (Schleussner et al., 2016) or a combination of scenarios (e.g. King et al., 2017) to extract  
71 climate information at specified GWLs, while others have used methods based on slower-  
72 warming or quasi-equilibrated climates (e.g. Lehner, Coats, et al., 2017; Wehner et al.,  
73 2018). While the Paris Agreement is not explicit, it has been argued that the aim is to stabilise  
74 global climate at a low GWL (Rogelj et al., 2017; Seneviratne et al., 2018), however, there is  
75 value in investigating transient warmer worlds given the current estimated rate of emissions

76 reductions (*NDC Synthesis Report* | UNFCCC, 2021) and high likelihood of continued  
77 warming.

78 It has long been known that transient and equilibrated climates differ in their pattern of  
79 warming, with transient climates characterised by greater land-ocean temperature differences  
80 (Manabe et al., 1991). Slow warming in high-latitude ocean regions occurs on centennial and  
81 even millennial timescales, such that stabilised climates exhibit a different warming pattern to  
82 transient climates (Geoffroy & Saint-Martin, 2014; Long et al., 2014). The effects of climate  
83 stabilisation have recently been elucidated further in multi-model experiments which  
84 highlight evolving patterns of warming over many centuries in simulations under fixed  
85 greenhouse gas concentrations (Huang et al., 2020; Rugenstein et al., 2019). Another recent  
86 study employed a time-slicing approach with a multi-model ensemble and found substantial  
87 differences between transient and quasi-equilibrium climates (King et al., 2020).

88 The majority of analyses examining effects of climate stabilisation have used fixed-forcing  
89 simulations (i.e. constant greenhouse gas concentrations) so that individual climate models  
90 exhibit different amounts of global warming associated with their varying climate sensitivity.  
91 To examine the effects of climate stabilisation at the Paris Agreement GWLs with a  
92 comparable set of transient model data requires a new approach. Here, we develop a  
93 framework for estimating differences in regional temperatures between transient and quasi-  
94 equilibrium climate states at the 1.5°C and 2°C GWLs informed by data across a wide range  
95 of simulated global temperatures. We use this approach to examine differences in the  
96 emergence of a human-caused climate change signal, adapting methods previously employed  
97 by Frame et al., (2017) and Hawkins et al., (2020) and applying them to the transient and  
98 quasi-equilibrium climates we generate.

99 The emergence of climate change signals in regional temperature and precipitation (Hawkins  
100 & Sutton, 2012; Lehner, Deser, et al., 2017; Mahlstein et al., 2011, 2012; Nguyen et al.,  
101 2018), climate extremes (Bador et al., 2016; Diffenbaugh & Scherer, 2011; Harrington et al.,  
102 2016; King et al., 2015), and other variables (Lo et al., 2020; Lyu et al., 2014) is useful as an  
103 index of how significantly the climate has changed since early-industrial times or is projected  
104 to change with future warming. The emergence of a climate change signal is often expressed  
105 as a time (i.e. the point when a novel climate has emerged from the variability of past  
106 climates) or a signal-to-noise ratio (S/N). Using S/N, we explore whether emergence of  
107 climate change signals differs between transient and quasi-equilibrium climates. While the  
108 emergence of climate change signals between high and low greenhouse gas emissions  
109 scenarios has been evaluated to some extent (e.g. Nguyen et al., 2018), climate stabilisation  
110 effects and associated changes in warming patterns have not previously been investigated in  
111 the context of climate change emergence.

## 112 **Data and Methods**

113 We used surface air temperature (“tas”) from ten models in the sixth phase of the Coupled  
114 Model Intercomparison Project (CMIP6; Eyring et al., 2016) to form transient and quasi-  
115 equilibrium warmer climates (Table S1). We use only greenhouse gas-forced simulations to  
116 build transient and quasi-equilibrium climates to eliminate regional effects of anthropogenic  
117 aerosols, ozone change, and land use/cover change on surface temperature patterns which  
118 exist in other simulations. We define transient climates using the 1%CO<sub>2</sub> simulations where  
119 carbon dioxide increases by 1% per year from a pre-industrial level resulting in a warming  
120 climate (Figure 1a) with generally a greater rate of warming than observed. The quasi-  
121 equilibrium climate is defined from pre-industrial control simulations (piControl) and abrupt  
122 CO<sub>2</sub> forcing experiments where carbon dioxide is halved (Abrupt-0.5xCO<sub>2</sub>), doubled  
123 (Abrupt-2xCO<sub>2</sub>) or quadrupled (Abrupt-4xCO<sub>2</sub>) relative to pre-industrial levels and then

124 simulations are run for typically 150 years. The 1%CO<sub>2</sub>, piControl, and Abrupt-4xCO<sub>2</sub>  
125 simulations form part of the CMIP6 Diagnostic, Evaluation and Characterization of Klima  
126 (DECK), while the Abrupt-0.5xCO<sub>2</sub> and Abrupt-2xCO<sub>2</sub> simulations are run as part of other  
127 projects (Good et al., 2016; Webb et al., 2017). The additional abrupt forcing simulations  
128 allow sampling from more of the distribution of global temperatures but limits the number of  
129 available models. The first 50 years of the abrupt forcing simulations are not used as these  
130 include a period of relatively rapid warming or cooling before the global-mean surface  
131 temperature (GMST) stabilises to some extent. The annual-average GMST trends from  
132 simulations chosen to make up the quasi-equilibrium climate are small, while trends from the  
133 1%CO<sub>2</sub> simulations are considerably larger on average (Figure 1a). We note that the abrupt  
134 forcings simulations are not in full equilibrium (which is why we refer to these simulations as  
135 *quasi-equilibrium*) as it takes centuries for the simulated climate to reach a new steady state  
136 (Charney et al., 1979; Rugenstein et al., 2019).

137 Model temperature data were interpolated to a common regular 2° grid. Seasonal-average  
138 temperatures were calculated for boreal summer (JJA) and winter (DJF). All global-average  
139 and local seasonal-average temperatures were calculated as anomalies from the average of  
140 piControl data for their respective model. To extract local climates at 1.5°C and 2°C GWLs, a  
141 relationship was derived between the 11-year smoothed (running mean) annual-average  
142 GMST and the seasonal-average temperature at each gridbox for the transient and quasi-  
143 equilibrium data from each model. An example is shown in Figures 1b and 1c for the gridbox  
144 over Paris in JJA in the CESM2 model for transient and quasi-equilibrium climates  
145 respectively. A fourth-order polynomial statistical fit was applied to the data to enable  
146 extraction of local climates at specified GWLs as it has residuals of similar magnitude  
147 between the transient and quasi-equilibrium ensembles, despite the clustered nature of the  
148 quasi-equilibrium data (Figures S1, S2). Several choices of fitting technique were considered

149 (discussion in Supplementary Information). The fourth-order polynomial is fit to the transient  
150 and quasi-equilibrium data separately and the associated equation is used to extract the  
151 gridbox seasonal-average temperature associated with the 1.5°C and 2°C GWLs. An analysis  
152 of sampling uncertainty effects on differences between transient and quasi-equilibrium  
153 climates was performed (Figure S3; discussion in Supplementary Information).

154 An attempt at evaluation of this process for generating transient and quasi-equilibrium  
155 climates is made by comparing recent observed warming, using the Berkeley Earth Surface  
156 Temperature dataset (Rohde et al., 2013; Rohde & Hausfather, 2020), with the statistical  
157 estimation of transient warming simulated by the climate models from 0.5°C to 1°C global  
158 warming (Figure S4; discussion in Supplementary Information).

159 The different emergent climate change signals between transient and quasi-equilibrium  
160 climates at 1.5°C and 2°C GWLs were explored as a way of elucidating the effects of the rate  
161 of global warming on local climates. The emergence of a climate change signal can be  
162 measured in different ways, such as Kolmogorov-Smirnov tests (Mahlstein et al., 2011) or  
163 probability ratios (Harrington et al., 2016), but the most commonly used method is S/N  
164 (Frame et al., 2017; Hawkins et al., 2020; Hawkins & Sutton, 2012; Nguyen et al., 2018).  
165 Signal and noise are calculated differently between studies; here the signal is simply the  
166 warming from the transient 1°C climate to the GWL in question as inferred from the fourth-  
167 order polynomial fit (similar to Frame et al. (2017)). The noise is the standard deviation of  
168 residuals from the fourth-order polynomial fit in the transient climate for values between  
169 0.5°C and 1°C global warming. This gives estimates of interannual climate variability that are  
170 relevant to recent climate. The S/N is then calculated for each model, and the ensemble-  
171 median for each location. The difference between S/N under transient and quasi-equilibrium  
172 climates at the same GWL is also computed. Smaller gridboxes at high latitudes likely inflate

173 noise relative to low latitudes (e.g. Fischer et al., 2013), but mapped differences in S/N  
174 between climate states are less affected by this property.

## 175 **Results**

176 The multi-model ensemble-median warming pattern is broadly similar between transient and  
177 quasi-equilibrium climates at 1.5°C and 2°C global warming (Figure 2) with pattern  
178 correlations exceeding 0.9 in both seasons. Warmer climates under both transient and quasi-  
179 equilibrium states exhibit greater warming over land than ocean (Joshi et al., 2008), and  
180 Arctic amplification is evident in DJF (Kim et al., 2016; Screen & Simmonds, 2010). There  
181 are, however, substantial and consistent differences between transient and quasi-equilibrium  
182 climates, especially in JJA (Figure 2i,j). Differences between transient and stabilised climates  
183 may arise from a number of sources, including the land-sea contrast evident in equilibrium vs  
184 transient runs in other settings (Dong et al., 2009; Joshi et al., 2008; Lambert et al., 2011).  
185 Land-sea contrasts arise from differences in effective heat capacity and slow heat transport in  
186 the ocean (e.g. Long et al., 2014, 2020), atmospheric lapse rate and relative humidity over  
187 land and ocean (Joshi et al., 2008), biological responses including stomatal resistance (Dong  
188 et al., 2009; Joshi & Gregory, 2008), and also differences over polar oceans (Collins et al.,  
189 2013). Here, the constraint of the same global warming level in transient and quasi-  
190 equilibrium states necessitates local differences in one region to be offset by differences of  
191 the opposite sign elsewhere. Consistent with previous literature, differences are evident over  
192 continental mid-latitude regions in the Northern Hemisphere where the model ensemble-  
193 median JJA-average temperature is at least 0.5°C greater in a transient climate than a quasi-  
194 equilibrium climate over large areas; this is the case at both 1.5°C and 2°C GWLs. In  
195 contrast, in the Southern Ocean, in particular, a quasi-equilibrium climate is warmer than a  
196 transient climate at the same GWL. In DJF (Figure 2k,l), differences between transient and  
197 quasi-equilibrium climates are less striking but remain substantial in some regions. The

198 overall pattern of differences shows strong seasonality. The strongest model agreement in the  
199 sign of the differences in transient and quasi-equilibrium temperatures tends to be in similar  
200 regions to where the largest differences in the ensemble-median are found. In at least nine of  
201 the ten climate models, in JJA there are large swathes of Northern Hemisphere land regions  
202 that are locally warmer in transient climates than quasi-equilibrium climates for the same  
203 GWL.

204 The differences between transient and quasi-equilibrium climates can also be contextualised  
205 against the current climate and the long-term goals of the Paris Agreement. Figure 3 shows  
206 the ensemble-median difference between transient and quasi-equilibrium climate states as a  
207 percentage of the difference between the transient 1°C climate (analogous to the recent  
208 climate) and the quasi-equilibrium climate at the 1.5°C and 2°C GWLs (the long-term Paris  
209 Agreement goals). Over much of North America and Eurasia differences exceed 100%  
210 meaning that the local difference in JJA-average temperatures between transient and quasi-  
211 equilibrium climates exceeds the local warming anticipated between the recent climate and  
212 the Paris Agreement 1.5°C GWL (Figure 3a). Over the Southern Ocean there are large areas  
213 where differences are below -50%, which indicates that the difference in both JJA- and DJF-  
214 average temperatures between quasi-equilibrium and transient climates locally accounts for  
215 more than half of the local warming associated with global warming from the recent climate  
216 to the long-term 1.5°C GWL (Figure 3a,b). These results highlight how large the difference  
217 between transient and quasi-equilibrium climate states can be relative to projected warming  
218 associated with low global warming targets. This effect weakens when applied to higher  
219 GWLs, but even relative to projected warming to the 2°C GWL, local differences between  
220 transient and quasi-equilibrium climates at the 2°C GWL remain substantial. Areas where the  
221 warming between the transient 1°C GWL and the quasi-equilibrium 1.5°C and 2°C GWLs is

222 very small, such as the North Atlantic, exhibit large percentage differences which are less  
223 meaningful.

224 The pattern of climate change emergence, as measured by the signal-to-noise, is also broadly  
225 similar between transient and quasi-equilibrium climate states with many low-latitude regions  
226 projected to experience S/N values greater than two (also known as “unfamiliar” climates  
227 relative to the recent climate; Frame et al. 2017) at 2°C global warming in either transient or  
228 quasi-equilibrium states (Figure 4). Higher S/N in low-latitude areas is a common feature in  
229 climate change emergence studies (Hawkins & Sutton, 2012; Mahlstein et al., 2011) and is  
230 primarily due to reduced interannual variability relative to higher latitudes.

231 Differences in S/N between transient and quasi-equilibrium climates are substantial due to  
232 differences in signal (S). Generally, land regions are projected to exhibit clearer emergence of  
233 local climate change signals under transient warming while oceans have higher S/N estimates  
234 in quasi-equilibrium climates for the same GWL. In boreal summer, S/N is greater by at least  
235 0.5 over large swathes of the Northern Hemisphere mid-latitudes. This represents a  
236 substantial effect of the rate of global warming on the projected detectability of changes in  
237 local climates up to the Paris Agreement GWLs. Over large areas of North America and  
238 Eurasia, summer-average temperatures would shift to becoming “unusual” (S/N between one  
239 and two; Frame et al. 2017) under a transient warming climate at the 1.5°C GWL, but under a  
240 quasi-equilibrium 1.5°C climate summer temperatures in these areas would remain similar to  
241 the recent climate (S/N less than one). The opposite is true for the Southern Ocean where  
242 climate change signals would continue to emerge as global climate stabilises at a given GWL.  
243 These S/N estimates illustrate that there will be perceptible differences in local climate for  
244 many parts of the world between transient and quasi-equilibrium climates.

245 **Discussion**

246 In this study we described a statistical framework for deriving comparable transient and  
247 quasi-equilibrium climate states at specified levels of global warming and under greenhouse  
248 gas-only forcings for the first time. We used this method to estimate differences between  
249 local temperatures in transient and quasi-equilibrium climates at the Paris Agreement GWLs  
250 of 1.5°C and 2°C above pre-industrial levels. We find substantial local differences between  
251 transient and quasi-equilibrium climates over some areas, particularly Northern Hemisphere  
252 mid-latitude land regions (warmer in a transient climate than a quasi-equilibrium state) and  
253 the Southern Ocean (cooler in a transient climate than a quasi-equilibrium state).

254 This study adds to others which show differences in temperature patterns between rapid-  
255 warming and steady-state climates (Armour et al., 2013; Geoffroy & Saint-Martin, 2014;  
256 Huang et al., 2020; King et al., 2020; Manabe et al., 1991; Rugenstein et al., 2019). Indeed, it  
257 is encouraging that differences between transient and quasi-equilibrium climates found in this  
258 study broadly resemble those seen in previous analyses despite being generated using a  
259 different method and dataset. This adds further weight to the need for decision-making based  
260 on climate projections to consider the path of global temperatures and rate of warming, as  
261 well as the amount of global warming. In particular, in heavily populated regions such as  
262 central Europe, parts of the Middle East, and east Asia, there is a strong indication that  
263 transient warming through a GWL is associated with much more local warming in boreal  
264 summer (broadly greater than 0.4°C) relative to a quasi-equilibrium climate at the same  
265 GWL. This results in very different possible local climates at the same amounts of global  
266 warming, so adaptation and mitigation planning informed by quantitative climate change  
267 information will need to account for the rate of global warming as well as the amount.  
268 Similarly, we find that the emergence of local climate changes differs between transient and  
269 quasi-equilibrium global climates. Stabilising the climate at the 1.5°C GWL would result in

270 substantially less perceptible temperature change in summer over North America and Eurasia  
271 than transient warming through the 1.5°C GWL.

272 While we believe this study to be helpful there are a number of caveats. As discussed in  
273 Supplementary Information, the choice of fitting method was a compromise, with no ideal  
274 technique identified, and evaluation of the method was challenging. The use of ten CMIP6  
275 models gives an estimate of model differences and uncertainty, but the sample size is  
276 constrained by the limited set of models with Abrupt-0.5xCO<sub>2</sub> and Abrupt-2xCO<sub>2</sub>  
277 simulations.

278 The use of a multi-model ensemble-median reduces effects of diverse model responses and  
279 internal variability in individual models affecting the results. Indeed, while most models  
280 produce broadly similar patterns of differences between transient and quasi-equilibrium  
281 worlds, there are rather different patterns in a minority of models (Figures S5,S6). No models  
282 can be justifiably removed from the ensemble due to difficulties with evaluation discussed  
283 previously. It is possible that outlier models with unusual patterns of temperature difference  
284 may have passed climate “tipping points” that are physically realistic and important to  
285 consider in projections (Lenton et al., 2019; Steffen et al., 2018).

286 There is a clear gap in our model experiments that necessitates methods such as the one  
287 applied here for developing analyses highlighting substantial differences between transient  
288 and quasi-equilibrium climate states at policy-relevant GWLs. New experiments would be  
289 beneficial if they involved participation of multiple modelling groups (given the large model  
290 differences shown in Figures S5, S6) and could follow the framework of Sigmond et al.,  
291 (2020), who ran multi-century simulations with some climate stabilisation.

292 In this study we discuss comparisons between *transient* and a *quasi-equilibrium* climate  
293 states. These terms can take on a host of different meanings. The transient climate analysed

294 here includes simulations mostly with slightly faster warming than the recent real-world trend  
295 (marked by cross in Figure 1a). By applying statistical fits on models separately, the effect of  
296 different models' transient climate responses on the pattern of differences between transient  
297 and quasi-equilibrium climate states may be examined, but no significant effect is identified  
298 (not shown). We refer to *quasi-equilibrium* climates rather than equilibrium climates as the  
299 simulations used are not run for long enough to reach a full equilibrium. Even after hundreds  
300 of years there are changes occurring in temperature patterns (Rugenstein et al., 2019) as some  
301 aspects of the earth system are particularly slow to respond to climate forcings. Indeed, ocean  
302 regions with detectable differences between transient and quasi-equilibrium states in this  
303 study (e.g. the Southern Ocean) experience larger local temperature changes as the planet  
304 moves towards full equilibrium (Rugenstein et al., 2019). Other aspects of the climate system  
305 are expected to differ between transient and quasi-equilibrium climate states, such as rainfall  
306 patterns (Burls & Fedorov, 2017; Sniderman et al., 2019), deep ocean temperatures (Gillett et  
307 al., 2011), vegetation (Heinze et al., 2019), and ice sheets and sea ice (Blackport & Kushner,  
308 2016; Hansen et al., 2013).

## 309 **Conclusions**

310 In this study we have developed a framework for the comparison of transient and quasi-  
311 equilibrium climates at a prescribed level of global warming under greenhouse-gas forcings.  
312 We have shown that there are substantial differences in local-, seasonal-average temperatures  
313 between transient and quasi-equilibrium climate states at the Paris Agreement GWLs and that  
314 these differences are large compared to the projected warming to the 1.5°C and 2°C GWLs.  
315 The emergence of local climate change signals in seasonal temperature also differs between  
316 transient and quasi-equilibrium climates pointing to a return to weaker local climate change  
317 impacts in Northern Hemisphere mid-latitude land regions if society achieves a steady-state  
318 climate at 1.5°C global warming as compared to a continued rapidly warming climate. Our

319 study demonstrates the need for regional climate projections at GWLs to account for the  
320 substantial influence of the rate of global warming to prevent misinformed decision-making.

### 321 **Data Availability statement**

322 All data used in this study are available to access in public repositories. The CMIP6 data are  
323 published here: <https://esgf-node.llnl.gov/projects/cmip6/> and data in this study were  
324 accessed through this ESGF and the National Computing Infrastructure ESGF in Australia  
325 (<https://esgf.nci.org.au/projects/esgf-nci/>). The BEST dataset is available publicly here: [http://](http://berkeleyearth.org/data/)  
326 [berkeleyearth.org/data/](http://berkeleyearth.org/data/).

### 327 **Acknowledgements**

328 A.D.K. was supported by the Australian Research Council (DE180100638). D.J.F., L.J.H.,  
329 and D.A.S. were supported by the Ministry of Business, Innovation and Employment of  
330 Aotearoa New Zealand through the Endeavour programme. S.K.M. was supported by a  
331 National Research Foundation of Korea (NRF) grant funded by the South Korean  
332 government (MSIT) (NRF-2018R1A5A1024958). A.G.P. was supported by the Regional  
333 and Global Model Analysis (RGMA) component of the Earth and Environmental System  
334 Modeling Program of the U.S. Department of Energy's Office of Biological & Environmental  
335 Research (BER) via National Science Foundation IA 1947282. J.M.K.S. was funded by  
336 Australian Research Council grant FL160100028 to Prof. Jon Woodhead. The authors  
337 acknowledge useful discussions with Ed Hawkins and Daniel Mitchell. We acknowledge the  
338 support of staff at the NCI facility in Australia and the World Climate Research Programme,  
339 which, through its Working Group on Coupled Modelling, coordinated and promoted CMIP6.  
340 We thank the climate modeling groups for producing and making available their model  
341 output, the Earth System Grid Federation (ESGF) for archiving the data and providing access,  
342 and the multiple funding agencies who support CMIP6 and ESGF.

343 **References**

- 344 Armour, K. C., Bitz, C. M., & Roe, G. H. (2013). Time-Varying Climate Sensitivity from  
345 Regional Feedbacks. *Journal of Climate*, 26(13), 4518–4534.  
346 <https://doi.org/10.1175/JCLI-D-12-00544.1>
- 347 Bador, M., Terray, L., & Boé, J. (2016). Emergence of human influence on summer record-  
348 breaking temperatures over Europe. *Geophysical Research Letters*, 43(1), 404–412.  
349 <https://doi.org/10.1002/2015GL066560>
- 350 Blackport, R., & Kushner, P. J. (2016). The Transient and Equilibrium Climate Response to  
351 Rapid Summertime Sea Ice Loss in CCSM4. *Journal of Climate*, 29(2), 401–417.  
352 <https://doi.org/10.1175/JCLI-D-15-0284.1>
- 353 Burls, N. J., & Fedorov, A. V. (2017). Wetter subtropics in a warmer world: Contrasting past  
354 and future hydrological cycles. *Proceedings of the National Academy of Sciences of the*  
355 *United States of America*, 114(49), 12888–12893.  
356 <https://doi.org/10.1073/pnas.1703421114>
- 357 Charney, J. G., Arakawa, A., James Baker, D., Bolin, B., Dickinson, R. E., Goody, R. M., et  
358 al. (1979). *CARBON DIOXIDE AND CLIMATE: A SCIENTIFIC ASSESSMENT*.
- 359 Collins, M., Knutti, R., Arblaster, J. M., Dufresne, J., Fichefet, T., Friedlingstein, P., et al.  
360 (2013). Long-term Climate Change: Projections, Commitments and Irreversibility. In  
361 G.-K. Stocker, T.F., D. Qin & V. B. and P. M. M. Plattner, M. Tignor, S.K. Allen, J.  
362 Boschung, A. Nauels, Y. Xia (Eds.), *Climate Change 2013: The Physical Science Basis.*  
363 *Contribution of Working Group I to the Fifth Assessment Report of the*  
364 *Intergovernmental Panel on Climate Change*. Cambridge University Press. Retrieved  
365 from [https://www.ipcc.ch/site/assets/uploads/2018/02/WG1AR5\\_Chapter12\\_FINAL.pdf](https://www.ipcc.ch/site/assets/uploads/2018/02/WG1AR5_Chapter12_FINAL.pdf)

366 Diffenbaugh, N. S., & Scherer, M. (2011). Observational and model evidence of global  
367 emergence of permanent, unprecedented heat in the 20th and 21st centuries. *Climatic*  
368 *Change*, 107(3), 615–624. <https://doi.org/10.1007/s10584-011-0112-y>

369 Dong, B., Gregory, J. M., & Sutton, R. T. (2009). Understanding land-sea warming contrast  
370 in response to increasing greenhouse gases. Part I: Transient adjustment. *Journal of*  
371 *Climate*, 22(11), 3079–3097. <https://doi.org/10.1175/2009JCLI2652.1>

372 Eyring, V., Bony, S., Meehl, G. A., Senior, C. A., Stevens, B., Stouffer, R. J., & Taylor, K. E.  
373 (2016). Overview of the Coupled Model Intercomparison Project Phase 6 (CMIP6)  
374 experimental design and organization. *Geoscientific Model Development*, 9(5), 1937–  
375 1958. <https://doi.org/10.5194/gmd-9-1937-2016>

376 Fischer, E. M., Beyerle, U., & Knutti, R. (2013). Robust spatially aggregated projections of  
377 climate extremes. *Nature Climate Change*, 3(12), 1033–1038.  
378 <https://doi.org/10.1038/nclimate2051>

379 Frame, D., Joshi, M. M., Hawkins, E., Harrington, L. J., & de Roiste, M. (2017). Population-  
380 based emergence of unfamiliar climates. *Nature Climate Change*, 7(6), 407–411. <https://doi.org/10.1038/nclimate3297>

382 Geoffroy, O., & Saint-Martin, D. (2014). Pattern decomposition of the transient climate  
383 response. *Tellus, Series A: Dynamic Meteorology and Oceanography*, 66(1), 23393.  
384 <https://doi.org/10.3402/tellusa.v66.23393>

385 Gillett, N. P., Arora, V. K., Zickfeld, K., Marshall, S. J., & Merryfield, W. J. (2011). Ongoing  
386 climate change following a complete cessation of carbon dioxide emissions. *Nature*  
387 *Geoscience*, 4(2), 83–87. <https://doi.org/10.1038/ngeo1047>

388 Good, P., Andrews, T., Chadwick, R., Dufresne, J. L., Gregory, J. M., Lowe, J. A., et al.

389 (2016). NonlinMIP contribution to CMIP6: Model intercomparison project for non-  
390 linear mechanisms: Physical basis, experimental design and analysis principles (v1.0).  
391 *Geoscientific Model Development*, 9(11), 4019–4028. [https://doi.org/10.5194/gmd-9-](https://doi.org/10.5194/gmd-9-4019-2016)  
392 4019-2016

393 Hansen, J., Sato, M., Russell, G., & Kharecha, P. (2013). Climate sensitivity, sea level and  
394 atmospheric carbon dioxide. *Philosophical Transactions of the Royal Society A:*  
395 *Mathematical, Physical and Engineering Sciences*, 371(2001).  
396 <https://doi.org/10.1098/rsta.2012.0294>

397 Harrington, L. J., Frame, D. J., Fischer, E. M., Hawkins, E., Joshi, M. M., & Jones, C. D.  
398 (2016). Poorest countries experience earlier anthropogenic emergence of daily  
399 temperature extremes. *Environmental Research Letters*, 11(5), 055007.  
400 <https://doi.org/10.1088/1748-9326/11/5/055007>

401 Haustein, K., Allen, M. R., Forster, P. M., Otto, F. E. L., Mitchell, D. M., Matthews, H. D., &  
402 Frame, D. J. (2017). A real-time Global Warming Index. *Scientific Reports*, 7(1), 15417.  
403 <https://doi.org/10.1038/s41598-017-14828-5>

404 Hawkins, E., & Sutton, R. (2012). Time of emergence of climate signals. *Geophysical*  
405 *Research Letters*, 39(1), n/a-n/a. <https://doi.org/10.1029/2011GL050087>

406 Hawkins, E., Frame, D., Harrington, L., Joshi, M. M., King, A. D., Rojas, M., & Sutton, R.  
407 (2020). Observed Emergence of the Climate Change Signal: From the Familiar to the  
408 Unknown. *Geophysical Research Letters*, 47(6). <https://doi.org/10.1029/2019GL086259>

409 Heinze, C., Eyring, V., Friedlingstein, P., Jones, C., Balkanski, Y., Collins, W., et al. (2019,  
410 July 10). ESD Reviews: Climate feedbacks in the Earth system and prospects for their  
411 evaluation. *Earth System Dynamics*. Copernicus GmbH. [https://doi.org/10.5194/esd-10-](https://doi.org/10.5194/esd-10-379-2019)  
412 379-2019

413 Huang, D., Dai, A., & Zhu, J. (2020). Are the transient and equilibrium climate change  
414 patterns similar in response to increased CO<sub>2</sub>? *Journal of Climate*, 33(18), 8003–8023.  
415 <https://doi.org/10.1175/JCLI-D-19-0749.1>

416 James, R., Washington, R., Schleussner, C.-F., Rogelj, J., & Conway, D. (2017).  
417 Characterizing half-a-degree difference: a review of methods for identifying regional  
418 climate responses to global warming targets. *Wiley Interdisciplinary Reviews: Climate*  
419 *Change*, 8(2), e457. <https://doi.org/10.1002/wcc.457>

420 Joshi, M. M., & Gregory, J. (2008). Dependence of the land-sea contrast in surface climate  
421 response on the nature of the forcing. *Geophysical Research Letters*, 35(24), L24802.  
422 <https://doi.org/10.1029/2008GL036234>

423 Joshi, M. M., Gregory, J. M., Webb, M. J., Sexton, D. M. H., & Johns, T. C. (2008).  
424 Mechanisms for the land/sea warming contrast exhibited by simulations of climate  
425 change. *Climate Dynamics*, 30(5), 455–465. <https://doi.org/10.1007/s00382-007-0306-1>

426 Kim, K.-Y., Hamlington, B. D., Na, H., & Kim, J. (2016). Mechanism of seasonal Arctic sea  
427 ice evolution and Arctic amplification. *The Cryosphere*, 10, 2191–2202.  
428 <https://doi.org/10.5194/tc-10-2191-2016>

429 King, A. D., Donat, M. G., Fischer, E. M., Hawkins, E., Alexander, L. V., Karoly, D. J., et al.  
430 (2015). The timing of anthropogenic emergence in simulated climate extremes.  
431 *Environmental Research Letters*, 10(9), 094015. [https://doi.org/10.1088/1748-](https://doi.org/10.1088/1748-9326/10/9/094015)  
432 [9326/10/9/094015](https://doi.org/10.1088/1748-9326/10/9/094015)

433 King, A. D., Karoly, D. J., & Henley, B. J. (2017). Australian climate extremes at 1.5 °C and  
434 2 °C of global warming. *Nature Climate Change*, 7(6).  
435 <https://doi.org/10.1038/nclimate3296>

436 King, A. D., Lane, T. P., Henley, B. J., & Brown, J. R. (2020). Global and regional impacts  
437 differ between transient and equilibrium warmer worlds. *Nature Climate Change*, *10*(1),  
438 42–47. <https://doi.org/10.1038/s41558-019-0658-7>

439 Lambert, F. H., Webb, M. J., & Joshi, M. M. (2011). The relationship between land-ocean  
440 surface temperature contrast and radiative forcing. *Journal of Climate*, *24*(13), 3239–  
441 3256. <https://doi.org/10.1175/2011JCLI3893.1>

442 Lehner, F., Coats, S., Stocker, T. F., Pendergrass, A. G., Sanderson, B. M., Raible, C. C., &  
443 Smerdon, J. E. (2017). Projected drought risk in 1.5°C and 2°C warmer climates.  
444 *Geophysical Research Letters*, *44*(14), 7419–7428.  
445 <https://doi.org/10.1002/2017GL074117>

446 Lehner, F., Deser, C., & Terray, L. (2017). Toward a New Estimate of “Time of Emergence”  
447 of Anthropogenic Warming: Insights from Dynamical Adjustment and a Large Initial-  
448 Condition Model Ensemble. *Journal of Climate*, *30*(19), 7739–7756.  
449 <https://doi.org/10.1175/JCLI-D-16-0792.1>

450 Lenton, T. M., Rockström, J., Gaffney, O., Rahmstorf, S., Richardson, K., Steffen, W., &  
451 Schellnhuber, H. J. (2019, November 28). Climate tipping points — too risky to bet  
452 against. *Nature*. Nature Research. <https://doi.org/10.1038/d41586-019-03595-0>

453 Lo, Y. T. E., Mitchell, D. M., Bohnenstengel, S. I., Collins, M., Hawkins, E., Hegerl, G. C.,  
454 et al. (2020). U.K. climate projections: Summer daytime and nighttime urban heat island  
455 changes in England’s major cities. *Journal of Climate*, *33*(20), 9015–9030.  
456 <https://doi.org/10.1175/JCLI-D-19-0961.1>

457 Long, S.-M., Xie, S.-P., Zheng, X.-T., & Liu, Q. (2014). Fast and Slow Responses to Global  
458 Warming: Sea Surface Temperature and Precipitation Patterns. *Journal of Climate*,  
459 *27*(1), 285–299. <https://doi.org/10.1175/JCLI-D-13-00297.1>

460 Long, S.-M., Xie, S. P., Du, Y., Liu, Q., Zheng, X. T., Huang, G., et al. (2020). Effects of  
461 ocean slow response under low warming targets. *Journal of Climate*, 33(2), 477–496.  
462 <https://doi.org/10.1175/JCLI-D-19-0213.1>

463 Lyu, K., Zhang, X., Church, J. A., Slangen, A. B. A., & Hu, J. (2014). Time of emergence for  
464 regional sea-level change. *Nature Climate Change*, 4(11), 1006–1010.  
465 <https://doi.org/10.1038/nclimate2397>

466 Mahlstein, I., Knutti, R., Solomon, S., & Portmann, R. W. (2011). Early onset of significant  
467 local warming in low latitude countries. *Environmental Research Letters*, 6(3), 034009.  
468 <https://doi.org/10.1088/1748-9326/6/3/034009>

469 Mahlstein, I., Portmann, R. W., Daniel, J. S., Solomon, S., & Knutti, R. (2012). Perceptible  
470 changes in regional precipitation in a future climate. *Geophysical Research Letters*,  
471 39(5), n/a-n/a. <https://doi.org/10.1029/2011GL050738>

472 Manabe, S., Stouffer, R. J., Spelman, M. J., & Bryan, K. (1991). Transient Responses of a  
473 Coupled Ocean–Atmosphere Model to Gradual Changes of Atmospheric CO<sub>2</sub>. Part I.  
474 Annual Mean Response. *Journal of Climate*, 4(8), 785–818.  
475 [https://doi.org/10.1175/1520-0442\(1991\)004<0785:TROACO>2.0.CO;2](https://doi.org/10.1175/1520-0442(1991)004<0785:TROACO>2.0.CO;2)

476 Masson-Delmotte, V., Zhai, P., Pörtner, H. O., Roberts, D., Skea, J., Shukla, P. R., et al.  
477 (2018). *Global warming of 1.5°C. An IPCC Special Report on the impacts of global*  
478 *warming of 1.5°C above pre-industrial levels and related global greenhouse gas*  
479 *emission pathways, in the context of strengthening the global response to the threat of*  
480 *climate change*,.

481 Mitchell, D., Achutarao, K., Allen, M., Bethke, I., Beyerle, U., Ciavarella, A., et al. (2017).  
482 Half a degree additional warming, prognosis and projected impacts (HAPPI):  
483 background and experimental design. *Geosci. Model Dev*, 10, 571–583.

484 <https://doi.org/10.5194/gmd-10-571-2017>

485 *NDC Synthesis Report | UNFCCC*. (2021). Retrieved from [https://unfccc.int/process-and-](https://unfccc.int/process-and-meetings/the-paris-agreement/nationally-determined-contributions-ndcs/nationally-determined-contributions-ndcs/ndc-synthesis-report#eq-5)

486 [meetings/the-paris-agreement/nationally-determined-contributions-ndcs/nationally-](https://unfccc.int/process-and-meetings/the-paris-agreement/nationally-determined-contributions-ndcs/nationally-determined-contributions-ndcs/ndc-synthesis-report#eq-5)

487 [determined-contributions-ndcs/ndc-synthesis-report#eq-5](https://unfccc.int/process-and-meetings/the-paris-agreement/nationally-determined-contributions-ndcs/nationally-determined-contributions-ndcs/ndc-synthesis-report#eq-5)

488 Nguyen, T. H., Min, S. K., Paik, S., & Lee, D. (2018). Time of emergence in regional

489 precipitation changes: an updated assessment using the CMIP5 multi-model ensemble.

490 *Climate Dynamics*, 51(9–10), 3179–3193. <https://doi.org/10.1007/s00382-018-4073-y>

491 Rogelj, J., Schleussner, C.-F., & Hare, W. (2017). Getting It Right Matters: Temperature

492 Goal Interpretations in Geoscience Research. *Geophysical Research Letters*, 44(20),

493 10,662–10,665. <https://doi.org/10.1002/2017GL075612>

494 Rohde, R. A., & Hausfather, Z. (2020). The Berkeley Earth Land/Ocean Temperature

495 Record. *Earth System Science Data*, 12(4), 3469–3479. [https://doi.org/10.5194/essd-12-](https://doi.org/10.5194/essd-12-3469-2020)

496 [3469-2020](https://doi.org/10.5194/essd-12-3469-2020)

497 Rohde, R. A., Muller, R., Jacobsen, R., Perlmutter, S., & Mosher, S. (2013). Berkeley Earth

498 Temperature Averaging Process. *Geoinformatics & Geostatistics: An Overview*, 01(02).

499 <https://doi.org/10.4172/2327-4581.1000103>

500 Rugenstein, M., Bloch-Johnson, J., Abe-Ouchi, A., Andrews, T., Beyerle, U., Cao, L., et al.

501 (2019). LongRunMIP: Motivation and Design for a Large Collection of Millennial-

502 Length AOGCM Simulations. *Bulletin of the American Meteorological Society*, 100(12),

503 2551–2570. <https://doi.org/10.1175/BAMS-D-19-0068.1>

504 Sanderson, B. M., Xu, Y., Tebaldi, C., Wehner, M., Neill, B. O. ', Jahn, A., et al. (2017).

505 Community Climate Simulations to assess avoided impacts in 1.5°C and 2°C futures.

506 *Earth System Dynamics*, 8, 827–847. <https://doi.org/10.5194/esd-2017-42>

507 Schaeffer, M., Hare, W., Rahmstorf, S., & Vermeer, M. (2012). Long-term sea-level rise  
508 implied by 1.5 °c and 2 °c warming levels. *Nature Climate Change*, 2(12), 867–870.  
509 <https://doi.org/10.1038/nclimate1584>

510 Schleussner, C.-F., Lissner, T. K., Fischer, E. M., Wohland, J., Perrette, M., Golly, A., et al.  
511 (2016). Differential climate impacts for policy-relevant limits to global warming: the  
512 case of 1.5 °C and 2 °C. *Earth System Dynamics*, 7(2), 327–351.  
513 <https://doi.org/10.5194/esd-7-327-2016>

514 Screen, J. A., & Simmonds, I. (2010). The central role of diminishing sea ice in recent Arctic  
515 temperature amplification. *Nature*, 464(7293), 1334–1337.  
516 <https://doi.org/10.1038/nature09051>

517 Seneviratne, S. I., Donat, M. G., Pitman, A. J., Knutti, R., & Wilby, R. L. (2016). Allowable  
518 CO2 emissions based on regional and impact-related climate targets. *Nature*, 529(7587),  
519 477–483. <https://doi.org/10.1038/nature16542>

520 Seneviratne, S. I., Rogelj, J., Séférian, R., Wartenburger, R., Allen, M. R., Cain, M., et al.  
521 (2018). The many possible climates from the Paris Agreement’s aim of 1.5 °c warming.  
522 *Nature*, 558(7708), 41–49. <https://doi.org/10.1038/s41586-018-0181-4>

523 Sigmond, M., Fyfe, J. C., Saenko, O. A., & Swart, N. C. (2020). Ongoing AMOC and related  
524 sea-level and temperature changes after achieving the Paris targets. *Nature Climate  
525 Change*, 10(7), 672–677. <https://doi.org/10.1038/s41558-020-0786-0>

526 Sniderman, J. M. K., Brown, J. R., Woodhead, J. D., King, A. D., Gillett, N. P., Tokarska, K.  
527 B., et al. (2019). Southern Hemisphere subtropical drying as a transient response to  
528 warming. *Nature Climate Change*. <https://doi.org/10.1038/s41558-019-0397-9>

529 Steffen, W., Rockström, J., Richardson, K., Lenton, T. M., Folke, C., Liverman, D., et al.

530 (2018, August 14). Trajectories of the Earth System in the Anthropocene. *Proceedings*  
531 *of the National Academy of Sciences of the United States of America*. National Academy  
532 of Sciences. <https://doi.org/10.1073/pnas.1810141115>

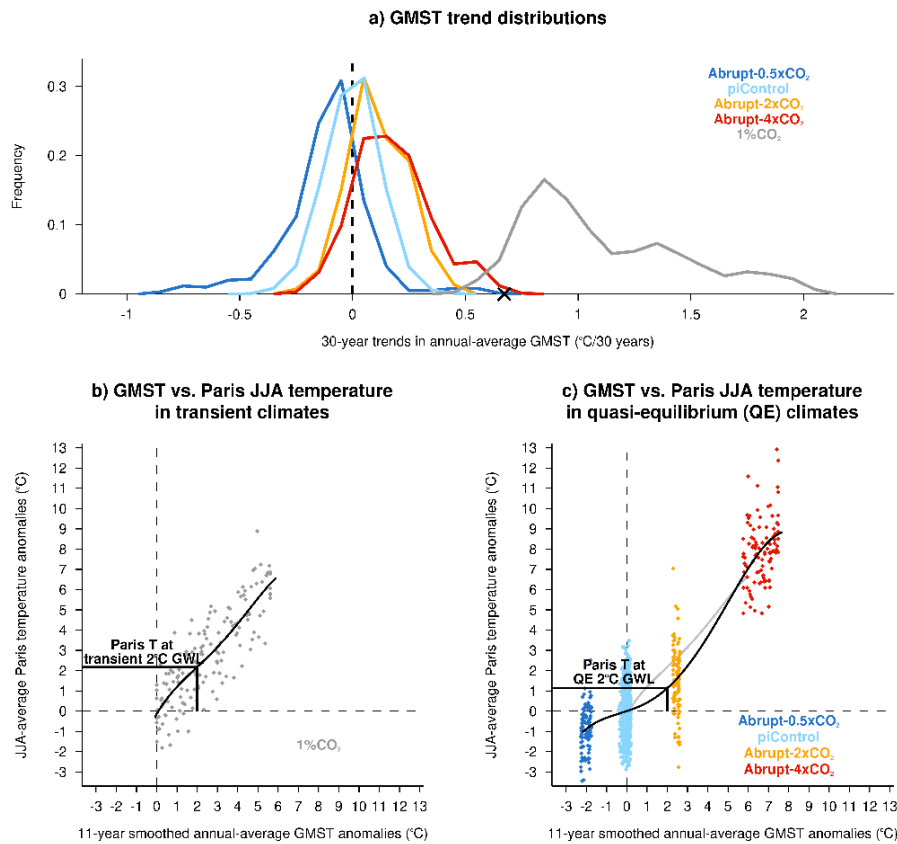
533 Tebaldi, C., & Knutti, R. (2018). Evaluating the accuracy of climate change pattern  
534 emulation for low warming targets. *Environmental Research Letters*, *13*(5), 055006.  
535 <https://doi.org/10.1088/1748-9326/aabef2>

536 Webb, M. J., Andrews, T., Bodas-Salcedo, A., Bony, S., Bretherton, C. S., Chadwick, R., et  
537 al. (2017). The Cloud Feedback Model Intercomparison Project (CFMIP) contribution to  
538 CMIP6. *Geoscientific Model Development*, *10*(1), 359–384.  
539 <https://doi.org/10.5194/gmd-10-359-2017>

540 Wehner, M., Stone, D., Mitchell, D., Shiogama, H., Fischer, E., Graff, L. S., et al. (2018).  
541 Changes in extremely hot days under stabilized 1.5 and 2.0 °C global warming scenarios  
542 as simulated by the HAPPI multi-model ensemble. *Earth System Dynamics*, *9*(1), 299–  
543 311. <https://doi.org/10.5194/esd-9-299-2018>

544

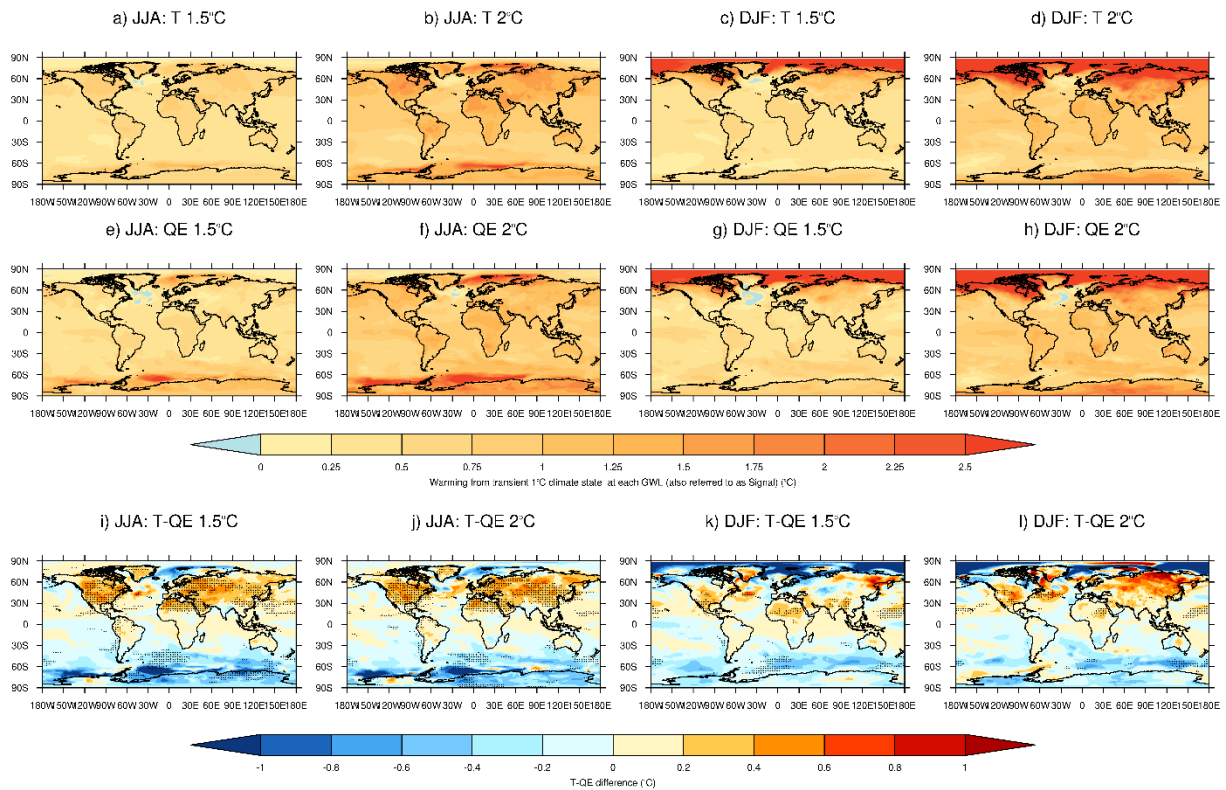
545



547

548 **Figure 1. GMST trends in greenhouse gas-forced simulations and examples of GMST**  
 549 **against Paris gridbox temperatures in transient and quasi-equilibrium warmer worlds.**

550 a) Statistical distributions of 30-year trends in annual-average GMST extracted from the  
 551 CMIP6 models in Table 1 for Abrupt-0.5xCO<sub>2</sub> (dark blue), piControl (light blue), Abrupt-  
 552 2xCO<sub>2</sub> (orange), Abrupt-4xCO<sub>2</sub> (red), and 1%CO<sub>2</sub> (grey) simulations. The black cross marks  
 553 the recent observed GMST trend from 1990-2020 in the BEST dataset. Scatter plots of 11-  
 554 year smoothed GMST against the Paris JJA-average gridbox temperatures in b) the transient  
 555 climate simulation and c) the ensemble of quasi-equilibrium simulations for the CESM2  
 556 model. In each graph the fourth-order polynomial fit is shown which is used to extract  
 557 GWLs, such as the 2°C GWL example shown. In c) the fourth-order polynomial fit for the  
 558 transient climate is shown in light grey for easier visual comparison with the quasi-  
 559 equilibrium fit.



560

561 **Figure 2. Constructed transient and quasi-equilibrium climates at Paris Agreement**

562 **GWLs and their differences.** Multi-model median warming pattern relative to transient 1°C

563 GWL extracted for a)-d) transient warmer worlds at a),c) 1.5°C global warming and b),d) 2°C

564 global warming for JJA and DJF respectively. Multi-model median warming pattern relative

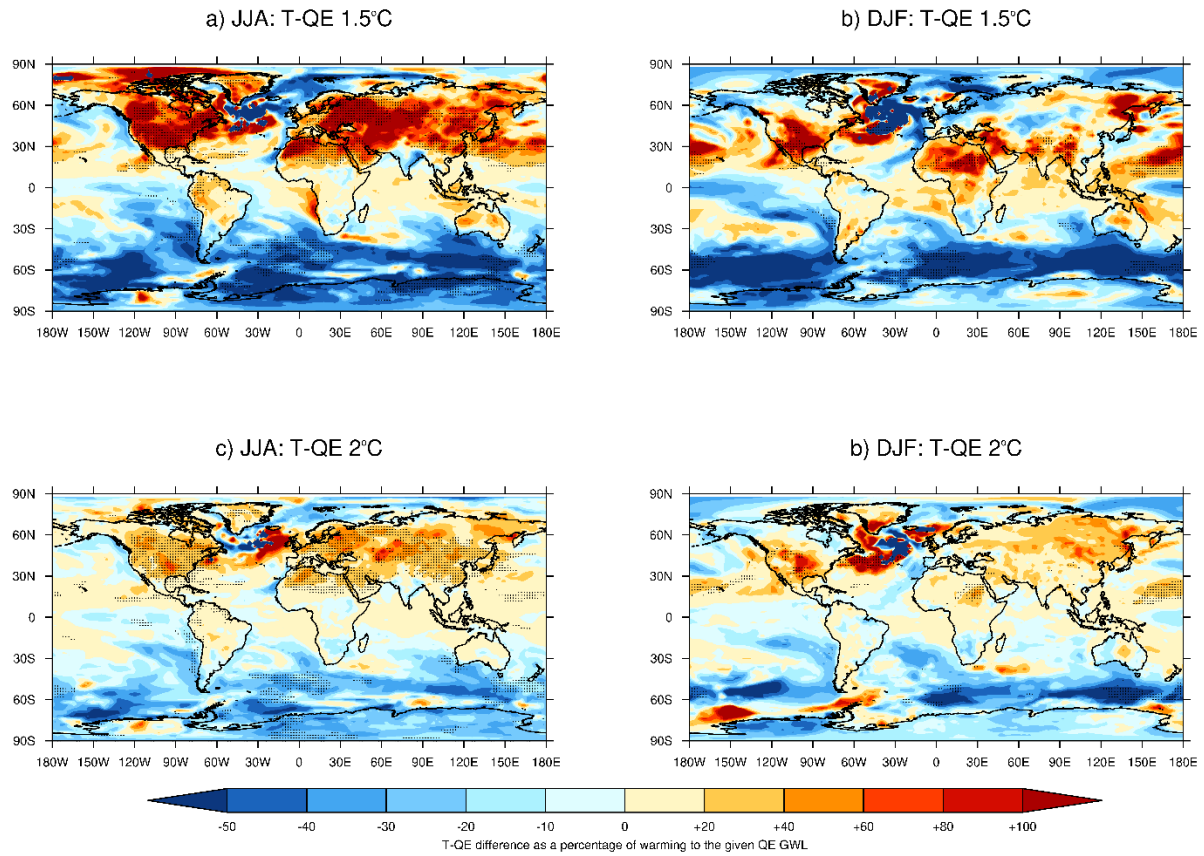
565 to transient 1°C GWL extracted for e)-h) quasi-equilibrium warmer worlds at e),g) 1.5°C

566 global warming and f),h) 2°C global warming for JJA and DJF respectively. Maps of the

567 multi-model median gridbox differences between transient and quasi-equilibrium climates at

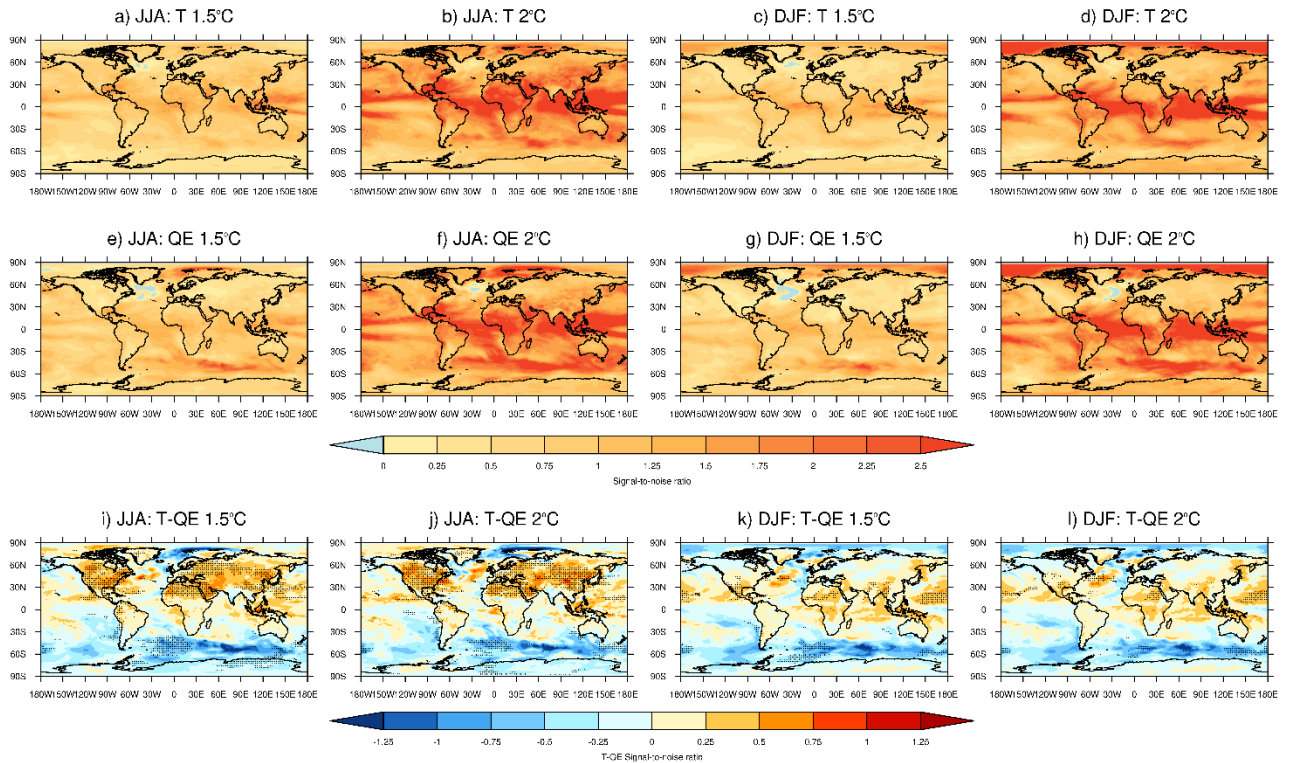
568 i),k) 1.5°C GWL and j),l) 2°C GWL in JJA and DJF respectively. Stippling in i)-l) indicates

569 at least nine out of ten model differences are of the same sign.



570

571 **Figure 3. Difference between transient and quasi-equilibrium climate states as a**  
 572 **percentage of projected warming.** Multi-model median maps of the difference between  
 573 transient and quasi-equilibrium seasonal-average temperatures at a),b) 1.5°C global warming  
 574 and c),d) 2°C global warming as a percentage of the projected warming from a transient 1°C  
 575 climate to a quasi-equilibrium climate at the same GWL. These maps are for a),c) JJA- and  
 576 b),d) DJF-average temperatures. Stippling indicates at least nine out of ten model differences  
 577 are of the same sign.



578

579 **Figure 4. Emergence of local climate change signals under different levels of global**  
 580 **warming for transient and quasi-equilibrium climate states.** The signal-to-noise of local  
 581 seasonal-average temperature changes in JJA and DJF at 1.5°C and 2°C global warming for  
 582 transient and quasi-equilibrium climate states. Differences in signal-to-noise ratios between  
 583 transient and quasi-equilibrium states are shown for g), h) JJA and i), j) DJF at 1.5°C and 2°C  
 584 global warming respectively. Stippling in i)-l) indicates at least nine out of ten model  
 585 differences are of the same sign (identical to Figure 3).